

REVIEW

SUBJECT COLLECTION: CELL MIGRATION

A minimal cell model for lamellipodia-based cellular dynamics and migration

Raj Kumar Sadhu^{1,*}, Aleš Iglič² and Nir S. Gov^{3,*}

ABSTRACT

One ubiquitous cellular structure for performing various tasks, such as spreading and migration over external surfaces, is the sheet-like protrusion called a lamellipodium, which propels the leading edge of the cell. Despite the detailed knowledge about the many components of this cellular structure, it is not yet fully understood how these components self-organize spatiotemporally to form lamellipodia. We review here recent theoretical works where we have demonstrated that membrane-bound protein complexes that have intrinsic curvature and recruit the protrusive forces of the cytoskeleton result in a simple, yet highly robust, organizing feedback mechanism that organizes the cytoskeleton and the membrane. This self-organization mechanism accounts for the formation of flat lamellipodia at the leading edge of cells spreading over adhesive substrates, allowing for the emergence of a polarized, motile 'minimal cell' model. The same mechanism describes how lamellipodia organize to drive robust engulfment of particles during phagocytosis and explains in simple physical terms the spreading and migration of cells over fibers and other curved surfaces. This Review highlights that despite the complexity of cellular composition, there might be simple general physical principles that are utilized by the cell to drive cellular shape dynamics.

KEY WORDS: Actin cytoskeleton, Cell migration, Cell shapes, Curved membrane proteins

Introduction

Eukaryotic cells intrinsically change their shape by deforming their membrane through local variations in the membrane composition and by reorganizing their underlying cytoskeleton. The many molecular components of the cell membrane and cytoskeleton involved in the cellular shape changes and motility have been, and are still being actively, exposed. Despite the extensive knowledge of the components of this system, an open question is to understand how the observed cellular shape dynamics emerge from the huge molecular complexity. This open challenge gives motivation for constructing simplified theoretical models that describe cellular shape dynamics using a general and simplified set of components. We review here one such theoretical approach.

Cells in our bodies have a myriad of different shapes depending on their function (Frey and Idema, 2021), from cells in the gut that are covered with microvilli (short protrusions) (Sauvanet et al., 2015) to the highly branched neurons. These shapes all involve deforming the flexible cell membrane into a variety of archetypal

forms, including cylindrical protrusions, such as filopodia (Mattila Pieta and Lappalainen, 2008), sheet-like extensions, such as lamellipodia (Innocenti, 2018), and cup-like invaginations, such as those occurring during endocytosis and phagocytosis (Flannagan et al., 2012), to name just a few common examples. These shapes can be rather static and maintain their form over long timescales (years), such as those of the stereocilia of the hair-cells in the inner ear (Naoy et al., 2008; Orly et al., 2015), whereas many are highly dynamic, forming and disassembling over timescales of minutes. Such dynamic shapes appear, for example, during development when cells differentiate, during cell motility (Bodor et al., 2020) and throughout the normal function of differentiated cells. One principal mechanism that allows cells to deform the membrane and achieve the desired shape is their cytoskeleton, mainly based on actin filaments (Pollard and Cooper, 2009; Salbreux et al., 2012). Polymerizing actin filaments allow cells to produce protrusive forces that push the bilayer membrane outwards (Mogilner and Oster, 2003; Liu et al., 2008), while the same actin network allows the cells to contract their membrane through the recruitment of myosin-II molecular motors (Koenderink and Paluch, 2018). An outstanding question in this field is how cells control the actin cytoskeleton in space and time so that polymerization and contractility self-organize where and when they should.

The underlying elements of the actin cytoskeleton that direct its polymerization to the cell membrane have been, and are still being, intensively explored. They include several families of actin polymerization promoter proteins that can form membrane-bound complexes (Welch and Mullins, 2002). Examples of such membrane-bound complexes include the Scar/WAVE complex (Machesky et al., 1999) and its binding partners, such as IRSp53 (also known as BAIAP2; Pipathsouk et al., 2021) and Abl (ABL1 in mammals; Zhu and Bhat, 2011) at the leading edge of lamellipodia. Typically, these actin polymerization promoters can be in an active or inactive form, with the activation occurring when they are part of the membrane-bound complex. Clearly this activation 'switch' allows the cells to control where actin polymerization occurs, by forming the active complexes (where actin polymerization occurs) in localized regions on the cell membrane. What determines the localization of these activated complexes on the cell membrane? One type of control can be exerted by external signaling, for instance chemokine molecules binding to membrane receptors could trigger a signaling cascade that locally activates membrane-bound actin polymerization promoters, inducing the polymerization of actin near the cell membrane (cortical actin). However, many cellular shapes form spontaneously, in the absence of external trigger or guidance.

One way to describe the dynamics of actin polymerization on the cell membrane, and how it forms dynamic patterns, has been in the form of reaction–diffusion (RD) equations. In this framework, several key components of the cortical actin network are described explicitly, including actin polymerization promoters, inhibitors of

¹Institut Curie, PSL Research University, CNRS, UMR 168, Paris 75005, France.

²Laboratory of Physics, Faculty of Electrical Engineering, University of Ljubljana, SI-1000 Ljubljana, Slovenia. ³Department of Chemical and Biological Physics, Weizmann Institute of Science, Rehovot 7610001, Israel.

*Authors for correspondence (raj-kumar.sadhu@curie.fr; nir.gov@weizmann.ac.il)

actin polymerization and both the polymerized and monomeric actin. The level of detail varies between these models, given that including the full complexity of the actin cytoskeleton and its associated proteins would make the models intractable (Mori et al., 2008; Bhattacharya et al., 2020; Driscoll et al., 2012; Bernitt et al., 2017). Nevertheless, these models have been successful, especially with respect to describing patterns of cortical actin polymerization and membrane composition such as actin waves propagating on the cell membrane, which also trigger lamellipodia protrusions (Taniguchi et al., 2013; Flemming et al., 2020). Most of these approaches so far have not included the deformation of the membrane as part of modeling the formation of spatiotemporal actin polymerization patterns. This is a valid approach for phenomena involving only small membrane deformations, such as those occurring on the basal surface of adhered cells. When membrane deformations are described by the RD framework, owing to the active forces (Campbell and Bagchi, 2018; Saito and Sawai, 2021), the membrane is usually described by a flexible substrate for the RD dynamics, but there is no explicit feedback whereby the membrane shape affects the chemical reactions that drive the RD dynamics (Ben Isaac et al., 2013). Explicit feedback between the membrane shape and the RD pattern formation has been considered in the absence of membrane deformations by active (actin-polymerization induced) forces (Wu and Liu, 2021; Tamemoto and Noguchi, 2020, 2021).

A few theoretical studies have addressed the three-dimensional shapes of isolated spreading (Serpelloni et al., 2021) and motile cells on surfaces of different curvatures (Link et al., 2023). One model contains a detailed description of the cellular mechanics and is based on the assumption of a central role for the nuclear dynamics and deformations in controlling the cell migration on the curved surface (Vassaux et al., 2019). A similar approach of modelling cell migration, where the process is dominated by the coupling between the nucleus and random peripheral protrusions (He and Jiang, 2017), produced migration patterns that were in qualitative agreement with observations (Song et al., 2015). Another model provides a simpler and more general description of three-dimensional cell migration in terms of an active fluid (Winkler et al., 2019), but its predictions were not systematically compared to experiments. A similar model was proposed to describe amoeboid cells moving along ridges, guided by a reaction-diffusion mechanism adapted from macropinocytic cup formation (Honda et al., 2021).

We review here another approach, where the membrane dynamics is driven by a population of curved membrane proteins, which recruit actin polymerization that exerts active, protrusive forces on the membrane. By ‘curved membrane proteins’ we mean in general a membrane-bound protein complex that has an intrinsic shape (Zimmerberg and Kozlov, 2006). Examples of intrinsically curved membrane-bound proteins include the BAR family (Liu et al., 2015). When such protein complexes form on the membrane, they tend to bend the membrane to conform to their intrinsic shape (McMahon and Boucrot, 2015; McMahon and Gallop, 2005; Alimohamadi and Rangamani, 2018).

In this model, active protrusive forces are exerted by the actin cytoskeleton (Mesarec et al., 2021), where the curved protein complexes (CMCs) direct the actin to polymerize and grow against the membrane at their locations. The CMC might contain proteins that act as nucleators of actin polymerization, such as WAVE proteins or WASp (also known as Was) (Takenawa and Miki, 2001; Pollitt and Insall, 2009; Stradal et al., 2004). There is evidence that curved membrane proteins form complexes with actin nucleators, especially at the leading edge of membrane protrusions, such as lamellipodia (Pipathsouk et al., 2021; Begemann et al., 2019).

When actin polymerization occurs near the membrane it exerts a pressure that pushes the membrane outwards, and the actin network backwards (retrograde flow) (Mogilner and Oster, 1996; Upadhyaya et al., 2003; Giardini et al., 2003; Carlsson, 2018). This is termed an ‘active’ force, to denote that it originates from processes that consume ATP and are therefore indicative that the living cell is not in thermal equilibrium. These forces convert chemical energy into mechanical work.

The combination of the intrinsic curvature of membrane-bound proteins and the protrusive forces of the cytoskeleton deforms the membrane and give rise to the emergence of different spontaneous shapes (Gov, 2018; Fošnarčič et al., 2019). We demonstrate that this coupling between curvature and cytoskeletal forces constitutes a ‘minimal cell’ model, which exhibits several fundamental cellular behaviors that resemble cell spreading (Sadhu et al., 2021, 2023a), phagocytosis (Sadhu et al., 2022) and cell migration. Although the numerical simulations allow us to calculate complex membrane dynamics and shapes in three-dimensional space, which are not easily (or at all) amenable to analytic description, the basic modeling scheme is very simple with respect to the number of components. In this framework, we do not attempt to describe the dynamics of actin polymerization at the level of the individual filaments, which can be cross-linked and undergo depolymerization. Models with a similar level of complexity of description have been proposed in other studies (Hu and Papoian, 2010). Although these models contain more realistic details of the actin dynamics, they are computationally very demanding, making the description of large membrane shapes difficult to achieve. In addition, their complexity renders understanding of the resulting dynamics very difficult.

We aim to keep our theoretical model simple, so that we can systematically explore, as well as gain deeper understanding of, the shapes and dynamics that our proposed coupling produces. We therefore avoid description in terms of specific proteins and instead denote their basic properties that are essential for our model, such as the intrinsic curvature of membrane proteins (or protein–lipid complexes) and the strength of the protrusive force actin polymerization exerts at their location on the membrane. The active force is exerted in our model at the locations of the curved membrane proteins in the direction of the locale outwards, normal to the membrane surface. This form of protrusive force, which acts as a local pressure field on the membrane, is most natural for describing branched actin networks, as opposed to highly oriented actin bundles (such as inside filopodia), and we therefore limit the discussion in this Review to cellular shapes driven by such networks. We start by introducing the theoretical model, before presenting a series of examples where we demonstrate how this model can help explain different forms of cellular dynamics, firstly, the spreading of a model minimal cell on a flat adhesive substrate, where we obtain different shapes and the emergence of a motile, polarized phenotype that resembles lamellipodia-driven cells. We then explore how the model minimal cell engulfs rigid adhesive particles, resembling phagocytosis, and demonstrate that its protrusions spontaneously coil on adhesive fibers, similar to the behavior of cellular protrusions. Finally, we utilize the model minimal cell to explore curvotaxis, the response of cell migration to curved surfaces (Schamberger et al., 2023; Pawluchin and Galic, 2022), which suggests that physical principles give rise to universal rules of cell migration on curved substrates.

Model

Our theoretical model is based on a coarse-grained continuum model (Fošnarčič et al., 2019; Sadhu et al., 2021; Drab et al., 2023),

where the flexible membrane of a vesicle is described as a two-dimensional surface that is built of triangles. The vertices of this triangulated surface are displaced by random Monte Carlo moves, driving the dynamics of the membrane (see Box 1 and figure therein). During the simulation, each displacement of the vertices is accepted if the total energy of the system decreases owing to this displacement (the energy terms are explained below). If the energy is increased by the displacement, the move is accepted according to the probability function that describes thermal fluctuations that drive such transient increases in the energy of the system. The use of a coarse-grained model means that we deal with length scales where the continuum description of the membrane is valid (i.e. larger than tens of nanometers), and do not include details of the molecular scale. In addition, we do not describe in this model the fluid flows that develop around (and in) the membrane as it moves and deforms. Such flows exert drag on the membrane and set the timescale for membrane shape deformations, and we therefore do describe the real timescale for the shape dynamics that we calculate. This means that the model describes the most energetically favorable shape changes that affect the dynamics, without the correct absolute timescales. We are able to compare relative times of shape changes by comparing their average number of Monte Carlo steps.

The energy terms that we consider in the model and their mathematical implementation are outlined below and in Box 1. We include the minimal energy terms, that necessarily exist in this system.

The first term accounts for the energy cost of bending the membrane. The lipid bilayer membrane minimizes its energy when the lipid head groups and the fatty tails have an optimal packing. This molecular arrangement endows the membrane with a preferred intrinsic (spontaneous) curvature. Unless the membrane composition has a large asymmetry between the two bilayer leaflets, this intrinsic curvature is close to zero, and the membrane prefers to be flat (Deserno, 2015; Safran, 2003). However, there are specific membrane-bound proteins that have a non-zero preferred curvature, and the membrane–protein complex minimizes its energy when its curved. The bending energy term is always positive (Helfrich, 1974).

We also consider that CMCs can bind to each other to form clusters and aggregates on the membrane. This binding is described as a negative energy term, which is therefore maximized when the CMC binds to form large clusters. This process, together with the spontaneous curvature of the CMC, can describe the spontaneous aggregation of the CMC to form small hemi-spherical buds, which can further aggregate to form ‘pearled’ clusters (Fig. 1). The buds have the exact spontaneous curvature of the CMC, thereby minimizing their bending energy, while their protein–protein binding energy stabilizes them against thermal fluctuations that act to break them apart. The formation of the pearled clusters maximizes this protein–protein binding energy by minimizing the number of isolated clusters. Such shapes might be observed in living cells for clusters of curved membrane proteins and nano-domains. Note that the membrane tension is not explicitly considered in most of our simulations, and we use a simpler condition that constrains the area changes per triangle, by setting minimal and maximal lengths per edge. This condition prevents pathological deformations and efficiently implements area conservation.

Given that cells can adhere to external surfaces, we consider an adhesion energy term. This energy represents the binding of the membrane to an external surface. It is therefore implemented as a negative energy increment whenever a vertex of the membrane is within a close distance to the surface. More complex adhesion rules can be implemented, but the simplest is to assume that the adhesion strength is uniform over all the membrane that is in proximity to the

surface (Sadhu et al., 2021). In addition, the membrane is prevented from moving across the external surface, which acts as a rigid barrier. The final energy term that we consider is a representation of the active force exerted by actin polymerization.

The active force, which pushes the membrane towards the outwards normal at each vertex that contains a CMC, represents the pressure that acts on the membrane owing to actin polymerization. This term is inherently non-equilibrium in the sense that it has no lower bound.

Actin polymerization is converted into an efficient protrusive force on the membrane (Mogilner and Oster, 1996) when the retrograde flow of the actin filaments experiences an effective friction with the substrate (Craig et al., 2015), mediated by specialized adhesion molecules (Gardel et al., 2010). We do not describe these adhesion molecules explicitly in our description, and simply allow each CMC to exert the same active force on the membrane, assuming that this friction affects all regions of the membrane equally. In addition, these adhesion molecules, and their binding–unbinding dynamics affects the movement of the cell membrane over the adhesive surface (Sackmann and Smith, 2014), exerting an effective friction that balanced the traction forces and determines the migration speed of the cell (DiMilla et al., 1991). We do not explicitly describe the dynamics of these adhesion molecules in our model.

Therefore, this model has only a few components. In the next sections, we present the different membrane shapes and dynamics that emerge in this model when the CMC vertices exert active protrusive forces, which represent the recruitment of actin polymerization, as well as adhesion to an external substrate.

Minimal cell spreading and migration on flat substrates

Many cell types are observed to spread and adhere to external rigid surfaces (Döbereiner et al., 2004; Cavalcanti-Adam et al., 2007). Such cells can either spread and remain stationary and adherent, or they become polarized and migrate on the surface. This process often involves the formation of a thin sheet-like protrusion around the cell edge, called a lamellipodium, which is driven by the formation of a branched actin network (Blanchoin et al., 2014; Le Clainche and Carlier, 2008), with the actin polymerization promoter, such as the WAVE complex, localized along the highly curved leading edge of the lamellipodium (Fritz-Laylin et al., 2017; Bieling and Rottner, 2023). As we show below, our model of a minimal cell describes a process that closely resembles the observed cell spreading by lamellipodia-like protrusions (Cuvelier et al., 2007; Xiong et al., 2010; Döbereiner et al., 2004).

When we let our minimal cell vesicle adhere and spread over a flat rigid surface, of uniform adhesiveness, we first find that this process is strongly affected by the presence of passive CMCs (i.e. in the absence of actin-driven forces; Fig. 2A). For the vesicle to spread, the adhesion energy gain has to offset the bending energy cost of forming a highly curved rim along the cell edge. The bending energy can prevent spreading on weakly adhered substrates; these are relevant to cells: in the absence of actin cytoskeleton activity, the bare cell membrane–substrate adhesion is usually weak and is insufficient to drive spreading over the surface (Guo et al., 2017). Given that cells need to be able to detach, move and remodel their adhesions, they do not form extremely strong, ‘super-glue’-like interactions with the substrate. We find that the highly curved, convex CMCs spontaneously aggregate along the curved rim of the spreading vesicle, thereby reducing the bending energy cost that acts to resist the spreading. Although this mechanism can be utilized by cells to facilitate spreading on weakly adhered substrates, it involves a large concentration of CMCs on the cell membrane.

When the CMCs recruit the protrusive force of actin polymerization, we find that they self-organize to form large aggregates along the cell rim, which drive robust spreading on the substrate, even at low CMC concentrations (Fig. 2B). The mechanism for this robust spreading is the positive feedback between the aggregation of the CMCs along the highly curved rim and the protrusive forces that they recruit, which push the membrane outwards and maintain the high curvature. The resulting adhered shape resembles adherent cells that are either round, with lamellipodia all along their edge (Szewczyk et al., 2013; Li et al., 2015), or elongated with mainly two competing lamellipodia protrusions at opposite ends of the cell. Note that adhered cells form stress fibers, which rely on and exert contractile forces on the cell membrane and external substrate (Schwarz and Safran, 2013). We do not include stress fibers in our current model. Our model captures the dynamics of the spreading observed in cells, including the ruffles that form at the

leading edge of the lamellipodia during the spreading process (Safran, 2003; Helfrich, 1974; Mogilner and Oster, 1996).

The elongated shapes arise in our model when the density of CMCs is so low that there are not sufficient CMCs to complete a continuous ring-like cluster along the leading edge of a circular spread vesicle (Fig. 2B). In this regime, we find that for intermediate actin force strength and strong adhesion, a polarized and motile phenotype emerges spontaneously in our model (Fig. 2C). This motile vesicle has a single, crescent cluster of CMCs along its leading edge, where the actin-driven forces are applied and maintain a sharp edge. The back of the vesicle is rounded, minimizing the bending energy of the membrane. We find that this motile vesicle resembles the shape of polarized motile cells, such as keratocytes. However, it is a rather fragile object – when our motile vesicle hits a barrier, or even due to spontaneous fluctuations, the leading-edge cluster of CMCs can break apart, and an immotile, elongated shape

Box 1. Model equations of the energy terms

We provide here a list of the energy terms that are calculated at each Monte Carlo displacement of the nodes of the triangulated membrane (see middle section of figure). The moves are accepted or rejected depending on the energy change due to this local displacement of a node, such that a move that decreases the energy is always accepted, while a move that increases the energy is accepted according to the probability given by the thermal distribution of states (Drab et al., 2023). In addition to the energy terms that we describe below, bond-flip events are implemented during the simulation (see right section of figure), which are accepted as long as the edge length is within some length bounds that maintain the topological stability of the calculation (Fošnarič et al., 2019). These bond flips result in effective fluidization of the triangulated surface, thereby facilitating the diffusion of the CMCs on the vesicle surface.

Bending energy

The lipid bilayer membrane minimizes its energy when the lipid head groups and the fatty tails have an optimal packing. This molecular arrangement endows the membrane with a preferred intrinsic (spontaneous) curvature (see left section of figure). Unless the membrane composition has a large asymmetry between the two bilayer leaflets, this intrinsic curvature is close to zero, and the membrane prefers to be flat. However, there are specific membrane-bound proteins that have a non-zero preferred curvature. We consider that these protein complexes are more rigid than the bilayer, and therefore the energy of the membrane can be written as a discretized version of the Helfrich form (Helfrich, 1974):

$$W_b = \frac{\kappa}{2} \sum_{i \text{ nodes}} (2h_i - c_{0,i})^2 A_i, \quad [1]$$

with κ the bending modulus, h_i the mean curvature and $c_{0,i}$ the spontaneous curvature of each node i , associated with area element A_i . The spontaneous curvature of the bare membrane nodes is usually taken to be zero ($c_{0,i}=0$), and for vertices that contain CMC, we will use here a high intrinsic convex curvature, $c_0 = 1/l_{\min}^{-1}$ (protruding outwards), where l_{\min} is the minimal allowed length of the edges in the triangulated surface (the length-scale in the problem). Eqn [1] has a minimum value of zero, when the local mean curvature of the membrane fits with the local intrinsic curvature of each of the vertices on the surface. When this mismatch is larger, a bending energy cost incurs.

Protein–protein binding energy

We consider that CMCs can bind to each other to form clusters and aggregates on the membrane (see left section of figure and Fig. 1). This is implemented by a binding energy between neighboring vertices on the triangulated surface of:

$$W_d = -\frac{w}{2} \sum_{i \text{ of CMP}} \sum_{nn \text{ of } i} \delta(\rho_i), \quad [2]$$

with the binding energy between nearest-neighbor (nn) CMC ($\rho_i=1$ for CMC, and $\rho_i=0$ for bare membrane vertex) of strength $w>0$ per CMC–CMC bond.

Membrane–substrate adhesion energy

Given that cells can adhere to external surfaces, we consider an adhesion energy term. For example, in the case of a flat adhesive surface, this amounts to (Sadhu et al., 2021):

$$W_{ad} = -E_{ad} \sum_{i \text{ nodes}} \delta(z_i - z_0 < \Delta z), \quad [3]$$

with energy E_{ad} per each adhered node, which is within a distance Δz of the substrate, where the rigid surface is located at $z=z_0$, and all the membrane vertices that are within a distance of $\Delta z=l_{\min}$ from this surface contribute an adhesion energy per unit area of $-E_{ad}$. In addition, the membrane is prevented from moving across the external surface, which acts as a rigid barrier.

Membrane tension energy

We can also calculate the explicit membrane tension using the following energy (Graziano et al., 2019):

$$W_s = \frac{\sigma}{2} \sum_{j \text{ triangles}} \left(\frac{a_j}{a_0} - 1 \right)^2, \quad [4]$$

where σ the effective membrane tension, and a_j, a_0 are the area and target area of each triangle.

In most of the simulations, we used a simpler condition that constrains the area changes per triangle, by setting minimal and maximal lengths per edge $l_{\min}, l_{\max}=1.7l_{\min}$. This condition prevents pathological deformations and efficiently implements area conservation.

Continued

Box 1. Continued

Active force that represents the force exerted by actin polymerization

The active force, that pushes the membrane towards the outwards normal (\hat{n}_i) at each node that contains a CMC (see right section of figure), is written as an additional energy (work) term:

$$\delta W_a = -F \sum_{i \text{ of CMC}} \vec{\delta r}_i \cdot \hat{n}_i, \tag{5}$$

such that the change in the energy of the system due to a small displacement of node i along the direction of the outwards normal $\vec{\delta r}_i \cdot \hat{n}_i$, is set by the force of strength F . This term is inherently non-equilibrium in the sense that it has no lower bound.

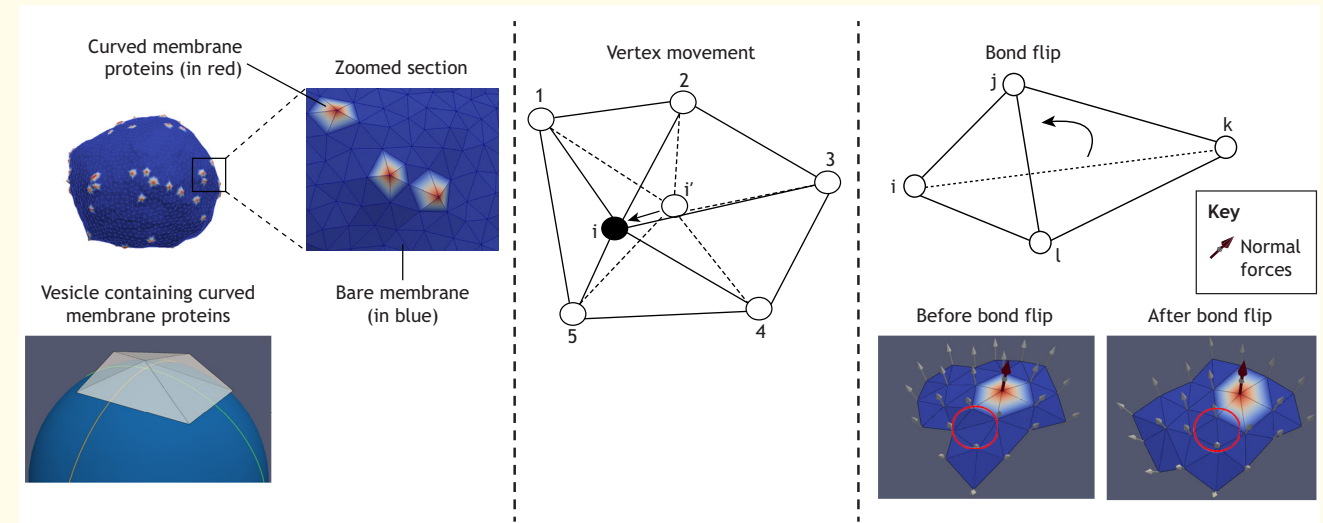


Figure adapted from Gov (2018) with permission from the Royal Society of Chemistry and from Schamberger et al. (2023) with permission from Elsevier.

emerges (Fig. 2D). Real cells are often observed to undergo similar events of leading-edge splitting (Andrew and Insall, 2007), but they have internal mechanisms to re-establish polarity, which we do not have in our current model (Maiuri et al., 2015).

Despite the simplicity of our model, it can be used to rationalize some puzzling experimental observations. For example, in the study of Spence et al. (2012) a type of mammalian breast cancer cells was found to be not very persistent and often had elongated shapes with

multiple and competing leading edges. Upon inactivation of some of the actin polymerization nucleators, these cells became crescent-shaped and persistent, with a single leading edge (Döbereiner et al., 2004). This puzzling observation can be explained with our model (Fig. 2C), in that for high actin-driven forces, elongated (non-motile) shapes dominate in our model, which correspond to the regular form of these cancer cells. When the magnitude of the active forces is reduced in the model, a motile vesicle appears,

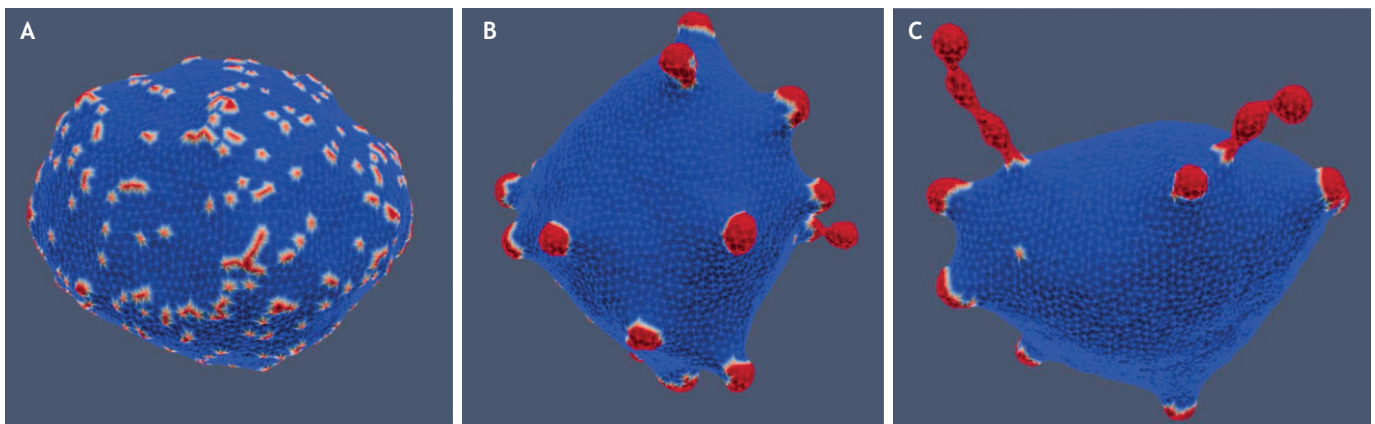


Fig. 1. Patterns of passive curved membrane proteins. Vesicle shapes and aggregates of curved membrane complexes, in the absence of active, actin-driven protrusive forces. The system initially starts as a random ‘gas’ of CMCs (shown in red) on the membrane (A), which diffuse and aggregate to form isolated hemispherical buds (B), at the spontaneous radius of curvature of the CMC. At longer times, the buds also diffuse and coalesce to form ‘pearled’ structures (C), which minimize the overall energy of the system. Figure adapted from Ravid et al. (2023), where it was published under a CC-BY 4.0 license. There is no inherent scale in the simulation, where lengths are given in units of the minimal edge length of the triangles that form the triangulated surface of the closed vesicle.

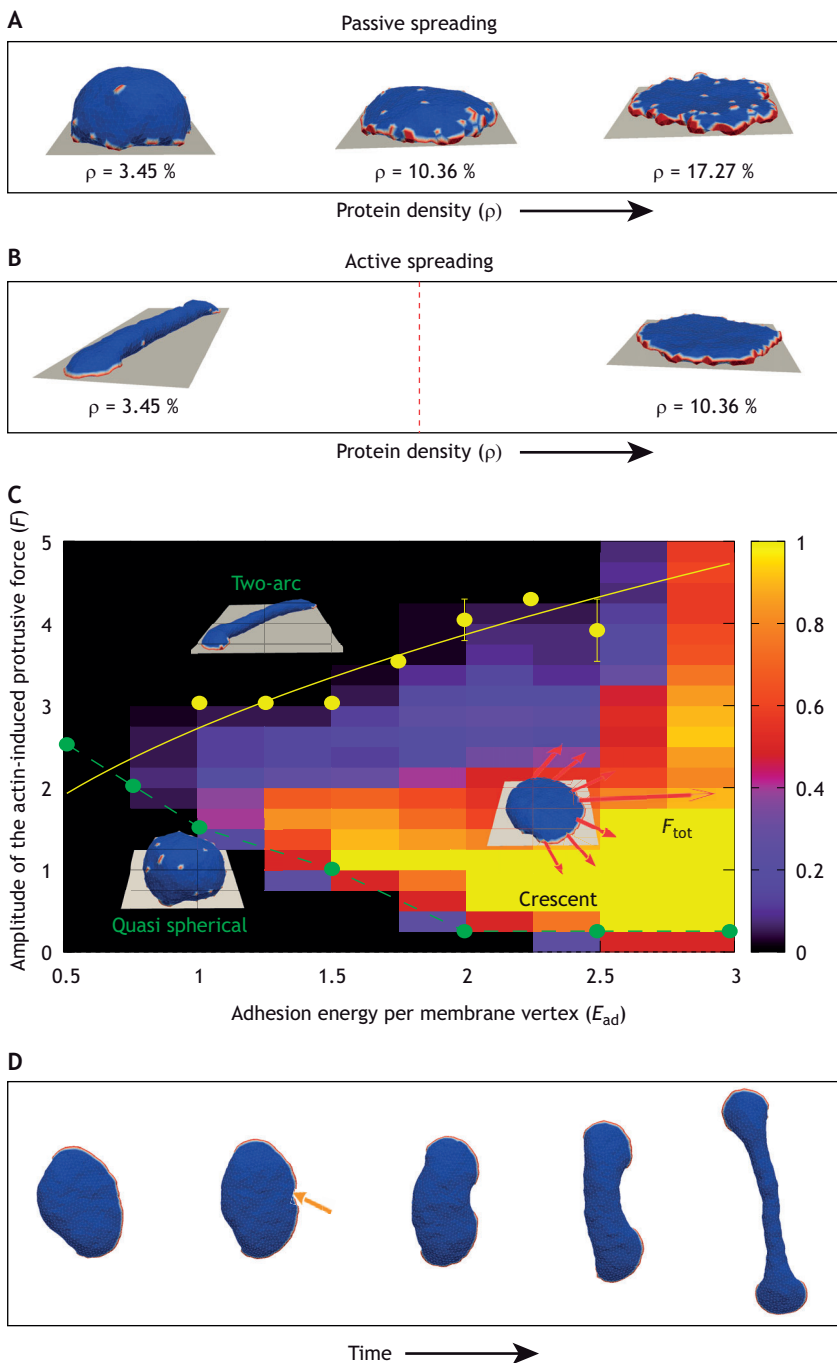


Fig. 2. Spreading and migration of a vesicle on flat substrate. (A) Spreading of a vesicle with passive CMCs (shown in red) with increasing CMC density (ρ). Shown here are snapshots for increasing CMC density on the vesicle surface ($\rho=3.45\%$, $\rho=10.36\%$ and $\rho=17.27\%$), and adhesion energy $E_{ad}=0.75 k_B T$. (B) Spreading of a vesicle with active CMCs with $F=4.0 k_B T/l_{min}$. For a small density of CMCs ($\rho=3.45\%$), where the passive CMCs do not induce spreading of the vesicle (A), the vesicle forms a two-arc-like shape with the active CMCs forming clusters at the two leading edges of the cellular protrusions. For larger density of CMC ($\rho=10.36\%$), the vesicle forms a flat, pancake-like shape, with the active CMCs forming a circular cluster along the rim of the spreading vesicle, exerting forces radially that act to spread the vesicle. Here, $E_{ad}=0.75 k_B T$ is used. (C) Phase diagram of the steady-state vesicle shape for active CMC with small density ($\rho=3.45\%$) as function of the (actin-induced) active protrusive force F and membrane–substrate adhesion energy E_{ad} . For a small E_{ad} and F , the vesicle forms a quasi-spherical like shape; for a small E_{ad} and large F , it usually forms the two-arc shape; for large E_{ad} , for a wide range of F (above the dashed green line and below the solid yellow line), the vesicle forms a crescent shape with the CMCs forming a single arc-like cluster at the leading edge, and the vesicle migrates on the flat substrate. The small red arrows indicate the active forces exerted by the active CMCs along the leading edge, with the total active force indicated by the large arrow. In this regime, the two-arc and crescent shapes coexist. (D) Spontaneous break-up of a motile crescent-like shape into a two-arc shape, following a random fluctuation that breaks the leading edge into two separate CMC clusters (indicated by the yellow arrow in the second snapshot). We use $E_{ad}=3.0 k_B T$ and $F=4 k_B T/l_{min}$ here. Other parameters are, $N=1447$, $\kappa=20 k_B T$, $w=1 k_B T$, $c_0=1 l_{min}^{-1}$. This figure is adapted from Sadhu et al. (2021), with kind permission of The European Physical Journal (EPJ).

corresponding to the motile cells that appeared for lower values of the actin polymerization activity.

Our model shows that the shape of a lamellipodium, in both adherent and motile cells, can spontaneously arise due to the coupling between convex CMCs and the protrusive forces of actin polymerization. This coupling leads to a self-organization process, maintaining the aggregation of CMCs along the lamellipodia-containing leading edge, giving rise to its distinct sheet-like morphology. This mechanism of lamellipodia formation, which we argue arises purely from a minimization of the system’s energy and work, is controlled in the cell by signaling networks. These biochemical controls allow the cell to spatially and temporally fine tune its response to different external stimuli.

Having established that our minimal cell model can recapitulate the spontaneous formation of lamellipodia during cell spreading, as well as the emergence of a motile phenotype, on a flat substrate, we next discuss how this model might explain the interactions of cells with curved surfaces.

Phagocytosis – the minimal cell engulfing solid objects

An *in vivo* example where a cell engages with a curved substrate, is during phagocytosis, the engulfment of a rigid particle by a cell (Flannagan et al., 2012; Cannon and Swanson, 1992; Kumari et al., 2010). Here, the cell membrane adheres to the particle and then spreads its membrane over it until complete engulfment occurs. During this process, there is a competition between the gain in adhesion energy and the cost of bending the membrane during

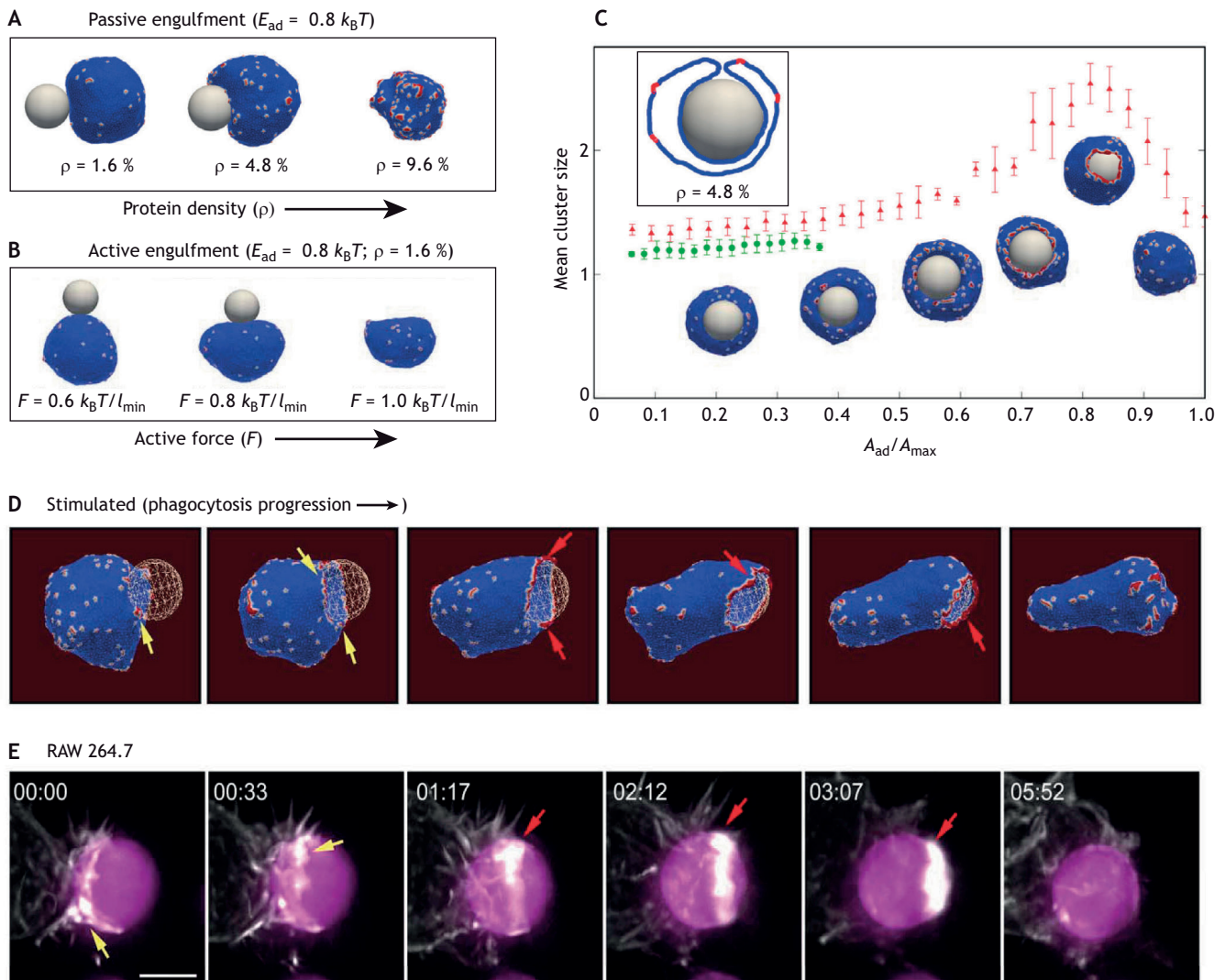


Fig. 3. Engulfment of particles by vesicles with passive and active CMCs. (A) Engulfment of spherical particles by vesicles with passive CMCs (in red) with $E_{ad}=0.8 k_B T$. The particle is engulfed as the density of CMCs (ρ) increases. Shown here are snapshots for $\rho=1.6\%$, $\rho=4.8\%$ and $\rho=9.6\%$. (B) Engulfment of spherical particles by vesicles with active CMCs with $E_{ad}=0.80 k_B T$ and $\rho=1.6\%$. The particle is finally engulfed as F increases, at a much lower density than for the passive CMCs (see A). Shown here are snapshots for $F=0.60 k_B T/l_{min}$, $F=0.80 k_B T/l_{min}$ and $F=1.0 k_B T/l_{min}$. (C) Mean cluster size (mean number of CMCs in a cluster) as a function of the engulfed area fraction, for both partial and complete engulfment cases with passive CMC (larger adhesion energy $E_{ad}=1 k_B T$). Error bars denote the standard deviation. Green circles are for $\rho=2.4\%$, where engulfment is blocked, and red triangles for $\rho=4.0\%$, where engulfment proceeds to completion. From this it is apparent that CMCs form a large cluster at the phagocytic cup rim, which drives the spreading of the membrane over the engulfed particle. The inset shows the cross sections of the vesicle membrane around the particle at the end of the engulfment process (for $\rho=4.8\%$), demonstrating that the cluster of CMCs spontaneously disperses from the phagocytic cup rim after the completion of the engulfment. (D,E) Clustering of active CMCs (representing the actin polymerization distribution) at the rim of the phagocytic cup and comparison with experimental observations. (D) Snapshots from a simulation (using $E_{ad}=1.5 k_B T$, $\rho=6.4\%$, and $F=1.0 k_B T/l_{min}$, $N=3127$) illustrating that the CMCs initially form fragmented clusters and arcs (yellow arrows), which are effective in pulling the membrane over the surface of the engulfed particle. At later times, the clusters form a continuous ring (red arrows), which spontaneously disperses after engulfment is complete. (E) Time-lapse sequences of maximum intensity projection images illustrating engulfment of immunoglobulin-G-coated polystyrene beads ($7 \mu\text{m}$ diameter, pink sphere) by RAW264.7 macrophage-like cell. Cells were transfected with mEmerald–Lifeact to label F-actin (white intensity). The yellow and red arrows indicate the fragmented actin arcs and the continuous actin ring at the rim of the phagocytic cup, corresponding to the same structures observed in the simulations shown in D. Scale bar: $5 \mu\text{m}$. Time is indicated in min: s. Adapted from Sadhu et al. (2022) with permission from the Royal Society of Chemistry.

engulfment. Similar to the case of spreading over a flat substrate (Fig. 2A), we find that the engulfment process can be facilitated by the presence of passive CMCs, which spontaneously aggregate along the highly curved leading edge (Fig. 3A,C) (Sadhu et al., 2021, 2022). This aggregation lowers the bending energy, such that the gain in adhesion energy overcomes the bending energy cost and the engulfment can be completed.

Phagocytosis is, however, an active process that is known to involve actin-mediated forces that push the engulfing

membrane forward (Mylvaganam et al., 2021). From numerous studies, we know that phagocytosis involves highly complex and dynamic rearrangements of the cytoskeleton, membrane shape deformations and protein aggregations (Niedergang and Chavrier, 2004). At present, there is no complete theoretical understanding of the dynamics of the self-organization of the membrane and the actin cytoskeleton, including the active forces it exerts during the engulfment process (Richards and Endres, 2017). However, we show that this

problem can be addressed using our theoretical model (Sadhu et al., 2022).

When CMCs recruit the protrusive actin-mediated forces, their aggregation along the leading edge is more robust, driving complete engulfment at lower density of CMCs compared to passive CMCs (Fig. 3A,B) and for non-spherical particles (Sadhu et al., 2022), which present a higher energy barrier for engulfment. In addition to lowering the bending energy barrier for engulfment, the actin-driven forces also contribute directly to the engulfment by pushing the leading edge of the membrane over the surface of the particle. The model predicts that this directed force is effective in driving the engulfment even when the cluster of CMCs at the leading edge does not form a complete ring but is composed of either a single partial arc or fragmented arcs (Fig. 3D). In these cases, a complete CMC ring usually forms at the later stages, as the engulfment progresses towards completion. These features, which appear in our model of fragmented actin clusters at the leading edge of the phagocytic cup, a complete actin ring as engulfment nears completion and final dispersal of the actin clustering after engulfment, have also been observed in recent experiments in cells using high-resolution imaging (Vorselen et al., 2021) (Fig. 3E).

Finally, as the engulfment is completed, the model predicts that the cluster of CMCs disperses spontaneously, as the narrow neck of membrane (our model does not allow fusion or fission of the membrane) does not have the mean curvature the CMCs require (Fig. 3D). The model therefore demonstrates that a complex biological process such as phagocytosis can be driven and coordinated using physical principles of minimization of energy and effective work. In the cell, these physical mechanisms are controlled by additional layers of biological signals, which determine when and where they are activated.

In the next two sections, we explore the prediction of our model for cells that spread over extended curved surfaces.

Minimal cell spreading over fibers

Cellular protrusions play important roles in exploring and sensing the extracellular environment during cell spreading and adhesion, cell migration and cell–cell interactions (Le Clairche and Carlier, 2008; Caswell and Zech, 2018). Lamellipodia protrusions enable cells to adhere and spread on fiber-like surfaces (Callens et al., 2020; Assoian et al., 2019; Koons et al., 2017), such as the fibers of the extracellular matrix (ECM) (Clark et al., 1982), as well as cylindrical protrusions of other cells, such as glial cells spreading over neighboring axonal extensions (Stadelmann et al., 2019; Djannatian et al., 2019). *In vitro* studies of cellular spreading and migration on fibers have shown the organization of different cell types on these fibers (Bade et al., 2017; Svitkina et al., 1995; Hwang et al., 2009; Meehan and Nain, 2014; Kennedy et al., 2017; Mukherjee et al., 2019; Guetta-Terrier et al., 2015), with cellular shape and motility found to depend on the curvature (diameter) of the fibers. These experiments have found indications for leading-edge cellular protrusions coiling (wrapping) around extracellular fibers, for instance in metastatic cancer cells (breast and ovarian), as well as in several other cell types (fibroblasts, epithelial and endothelial) (Koons et al., 2017; Mukherjee et al., 2019; Guetta-Terrier et al., 2015). However, the mechanisms that drive the tendency of the leading edge of cellular protrusions to rotate while cells are spreading on fibers is not understood at present.

Therefore, we have attempted to explain this behavior using our model, starting with an elongated, adherent vesicle that has two leading

edges on opposite ends (Fig. 4A) (Sadhu et al., 2023a). This configuration, which forms spontaneously in our model (Fig. 2B), resembles protrusions extended by cells on fibers (Koons et al., 2017; Mukherjee et al., 2019; Guetta-Terrier et al., 2015), with each protrusion having a lamellipodia-like leading edge, which in our model is composed of and driven by a cluster of CMCs. We find in our model that these protrusions spontaneously prefer to reorient along the circumferential direction, which gives rise to coiling-like motion (Fig. 4B) (Sadhu et al., 2023a). The origin of this preference is minimization of (mainly) bending and adhesion energy (Sadhu et al., 2023a). Using this insight, we used the model to predict behavior on fibers with a non-circular cross-section with sharp edges; here, the bending energy cost of coiling will prevail over the adhesion energy, and coiling or wrapping will be inhibited (Fig. 4C,D). This prediction was verified with experiments of cells spreading on fibers flattened to form ribbons with very narrow edges (Sadhu et al., 2023a), where the cellular protrusions do not coil around the fiber. As discussed in the previous examples above, despite the fact that a cell exhibits a highly complex ruffling dynamics at the leading edge, a simple model based on few physical principles can explain the tendency for coiling of the leading edge of a protrusion.

When a model vesicle spreads on a fiber, it can form a single leading edge and obtain the motile phenotype that we observed on the flat surface. The dynamics of such motile vesicles on curved surfaces is explored in the next section.

Minimal cell migrating over curved surfaces

Cells often migrate on curved surfaces inside the body, such as curved tissues, blood vessels, fibers of the extracellular matrix or cylindrical protrusions of other cells. Recent *in vitro* experiments provide clear evidence that motile cells are affected by the curvature of the substrate on which they migrate (Vassaux et al., 2019; Song et al., 2015; Assoian et al., 2019; Werner et al., 2020, 2018; Driscoll et al., 2014; Sanz-Herrera et al., 2009), preferring certain curvatures to others, a process termed curvotaxis. However, the origin and underlying mechanism of this curvature sensitivity are not well understood.

We focus here on two simple types of curved surfaces – a flat surface with a sinusoidal height undulation along one direction and a cylindrical fiber (as in the previous section). On both these surfaces, we can calculate the dynamic behavior of the model motile vesicle and compare it to the experimental observations (Sadhu et al., 2023b preprint).

Sinusoidal surface

A sinusoidal geometry has been experimentally investigated in several studies (Song et al., 2015; Pieuchot et al., 2018). For instance, the migration of T-lymphocytes has been studied on a surface with a unidirectional sinusoidal (wavy) height undulation (Song et al., 2015). Here, the cells were found to move axially (along the pattern) when inside the grooves (minima) of the surface topography, avoiding migration on the ridges (maxima) by crossing the ridges orthogonally. Indeed, our motile model vesicle exhibits this exact same qualitative behavior when it is small compared to the undulation wavelength (Fig. 5A,B) (Song et al., 2015; Sadhu et al., 2023b preprint). In contrast, when the undulation wavelength is smaller and the cell spans more than one groove or ridge, the vesicle can maintain stable motility orthogonal to the undulation pattern (Fig. 5C), while undergoing periodic changes in its speed.

Note that adherent cells, which are dominated by stress fibers and are weakly motile (such as fibroblasts), have been found to settle in the concave grooves or adhere aligned to the undulation axis (both on grooves and ridges) (Werner et al., 2018, 2019). In many

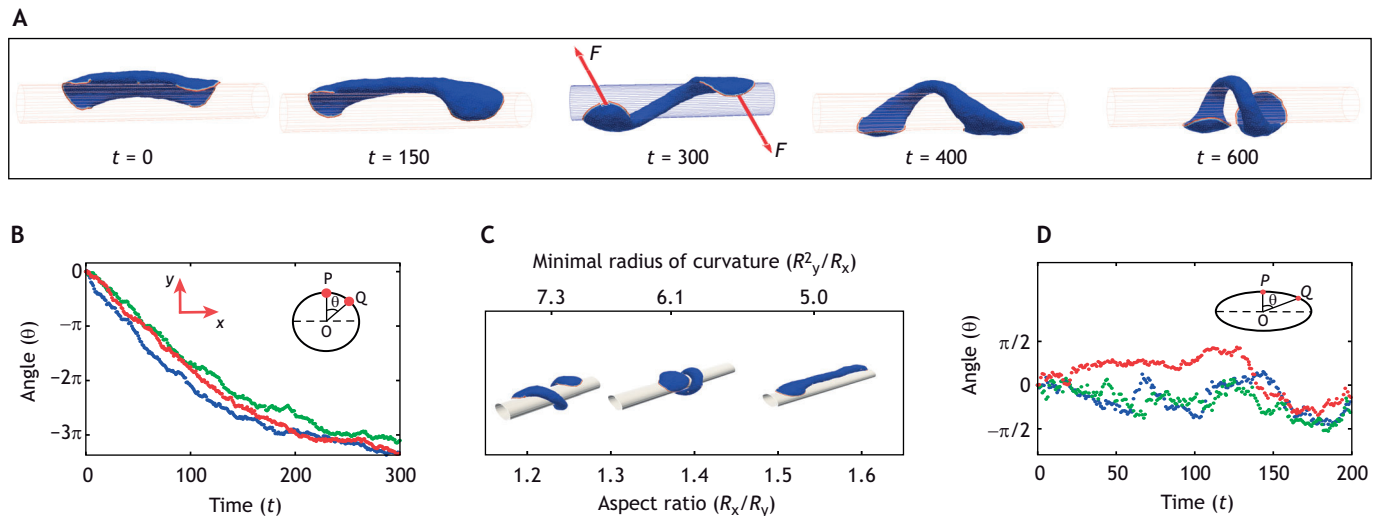


Fig. 4. Coiling of membrane protrusions around fibers. (A) Transition of a two-arc-shaped vesicle, which has two CMC clusters at opposite ends, from an axial (initial configuration) to a circumferential (coiling) orientation. Snapshots of the vesicle are shown at different times (in Monte Carlo units) as the coiling transition progresses. The red arrows on the 3rd inset show the direction of active forces that act on each of the two leading edges of the elongated vesicle by the CMC clusters that exert actin-induced protrusive forces. Here, $E_{ad}=2.0 k_B T$ is used. (B) Simulated angular displacement (θ) of the leading edges of the vesicle with time for the circular fiber ($R=10 l_{min}$). Different colors represent different realizations. The inset shows the definition of angular displacement (θ). Here, P and Q are the initial and final position, respectively, of a leading-edge protein on the x-y plane, and θ is the angular displacement between them. The initial linear angular displacement as function of time, over more than a full circle, indicates the highly directed angular coiling motion. Eventually the coiling motion stops as the membrane area of the vesicle is finite. The unit of time is 10^5 Monte Carlo (MC) steps. (C) Typical configurations of the simulated vesicles on fibers with elliptical cross sections. The coiling ceases as the aspect ratio of the fiber's elliptical cross section (R_x/R_y) increases above ~ 1.6 , as the bending energy cost to coil the membrane over the sharp edges of the fiber becomes prohibitively large. The circumference length of the elliptical cross section is kept constant, equal to the circumference of the circular cross-section with $R=10.0 l_{min}$. (D) Simulated angular displacement of the leading-edge of the vesicle as function of time for a fiber with an elliptical cross-section of aspect ratio 1.6 (as shown in the inset). Different colors represent different realizations. This demonstrates that the leading edges remain on the same side of the fiber and do not coil around the fiber. For (B-D) $E_{ad}=1.0 k_B T$, $\rho=2.4\%$ and $F=2 k_B T/l_{min}$ are used and the total number of vertices is $N=3127$. Figure adapted from Sadhu et al. (2023a), where it was published under a CC BY 4.0 license.

adherent cells, their direction of migration and axis of cellular elongation is determined by the competition between the bending energy of the stress fibers, deformation of the nucleus and the contractile forces applied by the stress fibers (Biton and Safran, 2009; Werner et al., 2020; Sanz-Herrera et al., 2009). These components are not included in our current model.

The agreement between the model and experiments on sinusoidal surfaces indicates that this form of curvotaxis can arise from only a few physical parameters. However, a sinusoidal surface has both positive and negative mean curvatures, which complicates the analysis of the resulting motion in terms of energy minimization. We therefore investigate next the migration over a cylindrical fiber, a surface with a uniform mean curvature.

Migration on a fiber

To simulate migration on a fiber, we started with our motile vesicle initially aligned along the axis of the fiber (Sadhu et al., 2023b preprint). The vesicle spontaneously rotates to align its motion along the circumferential direction (Fig. 5D) and continues to rotate around the fiber axis. The main energies that drive this reorientation, and stabilize the circumferential orientation, are the bending and adhesion energies. This is the same energy minimization process that gives rise to the coiling of elongated adherent vesicles (Fig. 4A) and can be used to explain the coiling dynamics of cellular protrusions on fibers. The increased adhesion in the circumferential orientation arises from the ability of the leading-edge cluster of CMCs to stretch the vesicle very effectively along the zero-curvature axial direction in this configuration.

Independently of our model, this predicted tendency of migrating cells to rotate around fibers has already been demonstrated

experimentally in a PhD thesis (Blum, 2015) for the orientation of *Dictyostelium discoideum* on a cylindrical fiber, clearly exhibiting the tendency of the cells to prefer the circumferential orientation (Fig. 5E,F) (Bade et al., 2017).

Taken together, we demonstrate here that a minimal cell model of a motile cell, based on only a few parameters and energy terms, is able to describe and explain several curvotaxis features of lamellipodia-driven cell migration on curved adhesive substrates. The curvotaxis features explained by the model, such as the tendency of motile cells to migrate aligned within grooves, avoid ridges and rotate around fibers, all arise owing to minimization of the adhesion and bending energies of the vesicle. Real cells contain numerous additional layers of complexity that our simple model does not, such as the effects of contractility, stress fibers and internal organelles (mainly the nucleus), which can all affect migration on curved substrates. Nevertheless, the agreement between the predictions of the model and the observations of curvotaxis in different types of migrating cells suggests that the simple energetic considerations in our model might indeed drive universal curvotactic features in lamellipodia-based motile cells.

Conclusions

These results from modeling a minimal cell demonstrate that complex cellular behavior might have underlying physical underpinnings, where energy and effective work minimization are the driving principle. As discussed above, a wide range of cellular shape dynamics and migration patterns can be obtained from a very simple model containing only a few components owing to the strong feedback between the intrinsic shape of the CMC and the active forces that deform the membrane. Our model shows that curved

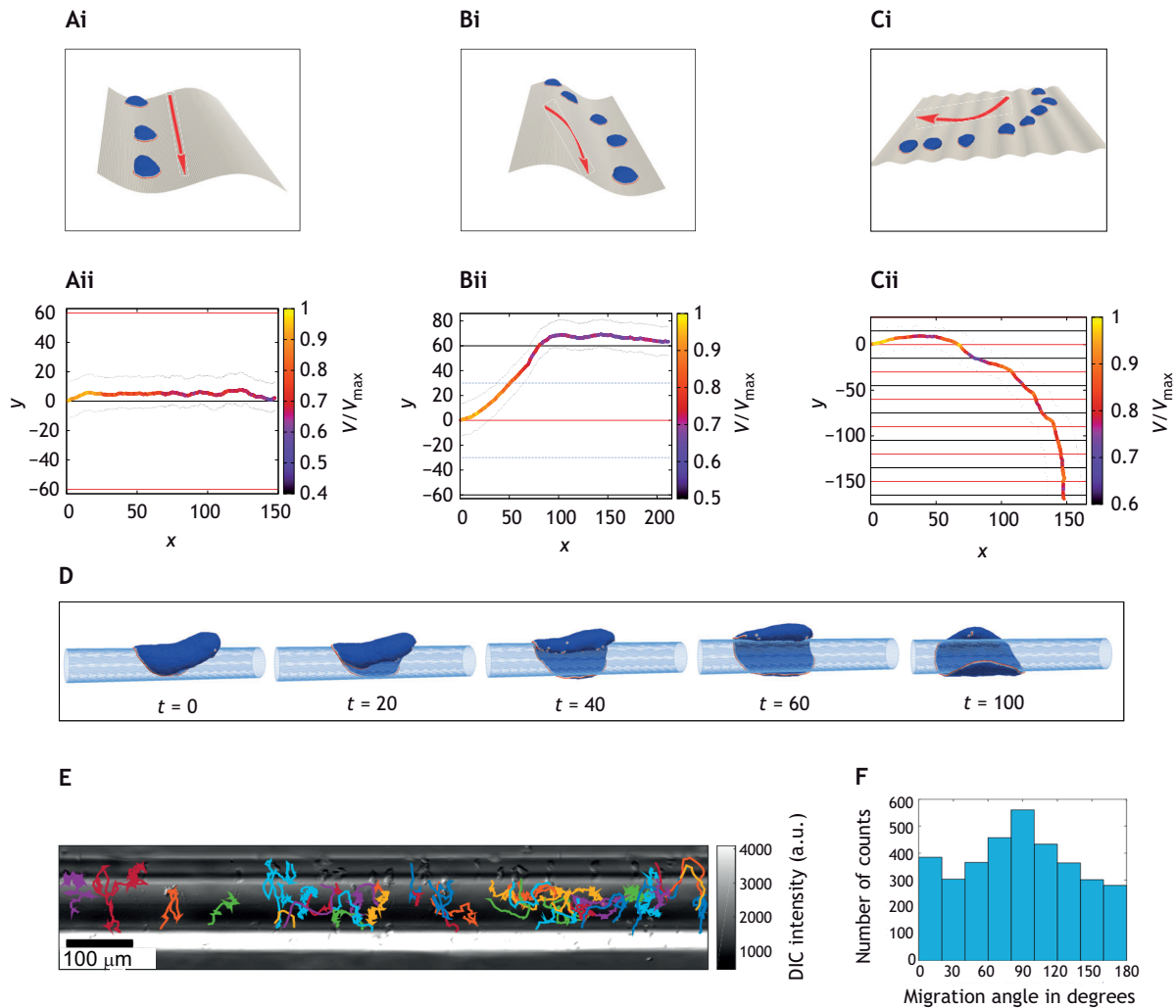


Fig. 5. Simulation of a motile vesicle migrating on curved surfaces and comparison with experiments. (Ai,Bi) A motile vesicle moving on a sinusoidal substrate with $\lambda/R_{\text{vesicle}} \gg 1$ (λ is the wavelength of the sinusoidal pattern and R_{vesicle} is the radius of the adhered motile vesicle). (A) The vesicle starts from the minimum of the sinusoidal groove, aligned initially with the groove, and continues its initial direction of migration. (B) The vesicle starts from the maximum of the sinusoidal ridge, aligned initially with the ridge, and migrates spontaneously to the minimum of one of the neighboring groove. In Ai and Bi, a sinusoidal height profile is used with an amplitude $10 I_{\text{min}}$, and wavelength $\lambda = 120 I_{\text{min}}$ (while $R_{\text{vesicle}} \sim 30 I_{\text{min}}$). (Ci) The vesicle moves on a sinusoidal substrate in the regime of $\lambda/R_{\text{vesicle}} \sim 1$. It starts from the maximum of the sinusoidal substrate and aligns with the pattern and then slowly changes its migration direction and migrates in an orthogonal direction to the sinusoidal pattern. Here, a sinusoidal height profile with an amplitude $2 I_{\text{min}}$, and $\lambda = 30 I_{\text{min}}$ is used. Other parameters for A–C are $N=607$, $E_{\text{ad}}=3 k_{\text{B}}T$, $\rho=4.9\%$ and $F=4 k_{\text{B}}T/l_{\text{min}}$. (Aii–Cii) The graphs underneath show the corresponding trajectories in the x-y plane for A to C, respectively, with the color indicating the speed of the vesicle. Note that the vesicle moves more slowly in the groove compared to when it moves over the ridge (Ai and Bi) while in Ci, it undergoes periodic velocity oscillations as it migrates up and down the ridges and grooves. (D) A vesicle migrating outside of a cylindrical fiber. The vesicle initially migrates in the axial orientation, but then spontaneously reorients, before finally assuming a circumferential orientation, which remains stable. Parameters used here are: $N=3127$, $R=10 I_{\text{min}}$, $E_{\text{ad}}=1.0$, $\rho=2.4\%$, $F=2.0 k_{\text{B}}T/l_{\text{min}}$. (E,F) Migrating *Dictyostelium discoideum* on cylindrical fiber (Blum, 2015). (E) Trajectories of different cells on the fiber. (F) Distribution of the direction of cell migration over the fiber from the trajectories shown in E. The clear peak at 90 degrees indicates the circumferential orientation of the migration. Figure adapted from Sadhu et al. (2023b, preprint). a.u., arbitrary units.

membrane complexes that recruit the forces exerted by actin polymerization constitute a versatile mechanism for spontaneous pattern formation on the cellular level, which are able to drive numerous cellular shapes and dynamics that correspond to observed cellular behavior (Graziano et al., 2019). This physical mechanism is regulated in the cell, in space and time, by additional layers of biological complexity and signaling networks.

This approach also demonstrates the power of simple physical models in exposing very general mechanisms for the self-organization of the cytoskeleton, which are not cell type specific, but are often obscured by biochemical details. Gaining such general understanding greatly advances our ability to control and predict the

dynamics of cells over a wide range of cell types and cellular dynamics. Such models can also motivate experiments aimed at recreating a similar minimal cell *in vitro* (Streicher et al., 2009). A recent extension of the work reviewed here demonstrates that the minimal cell model might explain the responses of lamellipodia-driven motile cells to shear flow (Sadhukhan et al., 2023). Future extensions of the work presented here will need to explore additional factors, such as the effects of CMCs with anisotropic shapes (Pipathsouk et al., 2021; Kabaso et al., 2012; Mesarec, et al., 2023) and mixtures of CMCs of several types of curvatures (both convex and concave) (Ravid et al., 2023). We reviewed here modeling cellular shapes driven by branched-actin networks, such

as lamellipodia and ruffles, but this framework can also be extended to describe the effects of actin filament bundling, which occurs inside finger-like filopodia protrusions (Ravid et al., 2023).

Acknowledgements

N.S.G. is the incumbent of the Lee and William Abramowitz Professorial Chair of Biophysics.

Competing interests

The authors declare no competing or financial interests.

Funding

Our work in this area is made possible in part by the historic generosity of the Harold Perlman Family. N.S.G. acknowledges support by the Ben May Center for Theory and Computation, the Ilse Katz Institute for Material Sciences and Magnetic Resonance Research and the Israel Science Foundation (Grant no. 207/22). A.I. was supported by the Slovenian Research Agency (ARRS) through the grants nos J3-3066 and J2-4447 and program no. P2-0232. R.K.S. acknowledges the support from Agence Nationale de la Recherche (ANR-19-CE11-0002-03).

References

- Alimohamadi, H. and Rangamani, P.** (2018). Modeling membrane curvature generation due to membrane–protein interactions. *Biomolecules* **8**, 120. doi:10.3390/biom8040120
- Andrew, N. and Insall, R. H.** (2007). Chemotaxis in shallow gradients is mediated independently of PtdIns 3-kinase by biased choices between random protrusions. *Nat. Cell Biol.* **9**, 193–200. doi:10.1038/ncb1536
- Assoian, R. K., Bade, N. D., Cameron, C. V. and Stebe, K. J.** (2019). Cellular sensing of micron-scale curvature: a frontier in understanding the microenvironment. *Open Biol.* **9**, 190155. doi:10.1098/rsob.190155
- Bade, N. D., Kamien, R. D., Assoian, R. K. and Stebe, K. J.** (2017). Curvature and Rho activation differentially control the alignment of cells and stress fibers. *Sci. Adv.* **3**, e1700150. doi:10.1126/sciadv.1700150
- Begemann, I., Saha, T., Lamparter, L., Rathmann, I., Grill, D., Golbach, L., Rasch, C., Keller, U., Trappmann, B., Matis, M. V. et al.** (2019). Mechanochemical self-organization determines search pattern in migratory cells. *Nat. Phys.* **15**, 848–857. doi:10.1038/s41567-019-0505-9
- Ben Isaac, E., Manor, U., Kachar, B., Yochelis, A. and Gov, N. S.** (2013). Linking actin networks and cell membrane via a reaction-diffusion-elastic description of nonlinear filopodia initiation. *Phys. Rev. E* **88**, 022718. doi:10.1103/PhysRevE.88.022718
- Bernitt, E., Döbereiner, H.-G., Gov, N. S. and Yochelis, A.** (2017). Fronts and waves of actin polymerization in a bistability-based mechanism of circular dorsal ruffles. *Nat. Commun.* **8**, 15863. doi:10.1038/ncomms15863
- Bhattacharya, S., Banerjee, T., Miao, Y., Zhan, H., Devreotes, P. N. and Iglesias, P. A.** (2020). Traveling and standing waves mediate pattern formation in cellular protrusions. *Sci. Adv.* **6**, eaay7682. doi:10.1126/sciadv.aay7682
- Bieling, P. and Rottner, K.** (2023). From WRC to Arp2/3: Collective molecular mechanisms of branched actin network assembly. *Curr. Opin. Cell Biol.* **80**, 102156. doi:10.1016/j.ceb.2023.102156
- Biton, Y. Y. and Safran, S. A.** (2009). The cellular response to curvature-induced stress. *Phys. Biol.* **6**, 046010. doi:10.1088/1478-3975/6/4/046010
- Blanchoin, L., Boujemaa-Paterski, R., Sykes, C. and Plastino, J.** (2014). Actin dynamics, architecture, and mechanics in cell motility. *Physiol. Rev.* **94**, 235–263. doi:10.1152/physrev.00018.2013
- Blum, C.** (2015). Curvotaxis and pattern formation in the actin cortex of motile cells. PhD thesis, Georg-August Universität, Göttingen, Germany.
- Bodor, D. L., Pönisch, W., Endres, R. G. and Paluch, E. K.** (2020). Of cell shapes and motion: the physical basis of animal cell migration. *Dev. Cell* **52**, 550–562. doi:10.1016/j.devcel.2020.02.013
- Callens, S. J. P., Uyttendaele, R. J. C., Fratila-Apachitei, L. E. and Zadpoor, A. A.** (2020). Substrate curvature as a cue to guide spatiotemporal cell and tissue organization. *Biomaterials* **232**, 119739. doi:10.1016/j.biomaterials.2019.119739
- Campbell, E. J. and Bagchi, P.** (2018). A computational model of amoeboid cell motility in the presence of obstacles. *Soft Mat.* **14**, 5741–5763. doi:10.1039/C8SM00457A
- Cannon, G. J. and Swanson, J. A.** (1992). The macrophage capacity for phagocytosis. *J. Cell Sci.* **101**, 907–913. doi:10.1242/jcs.101.4.907
- Carlsson, A. E.** (2018). Membrane bending by actin polymerization. *Curr. Opin. Cell Biol.* **50**, 1–7. doi:10.1016/j.ceb.2017.11.007
- Caswell, P. T. and Zech, T.** (2018). Actin-based cell protrusion in a 3D matrix. *Trends Cell Biol.* **28**, 823–834. doi:10.1016/j.tcb.2018.06.003
- Cavalcanti-Adam, E. A., Volberg, T., Micoulet, A., Kessler, H., Geiger, B. and Spatz, J. P.** (2007). Cell spreading and focal adhesion dynamics are regulated by spacing of integrin ligands. *Biophys. J.* **92**, 2964–2974. doi:10.1529/biophysj.106.089730
- Clark, R. A. F., Lanigan, J. M., Dellapelle, P., Manseau, E., Dvorak, H. F. and Colvin, R. B.** (1982). Fibronectin and fibrin provide a provisional matrix for epidermal cell migration during wound reepithelialization. *J. Invest. Dermatol.* **79**, 264–269. doi:10.1111/1523-1747.ep12500075
- Craig, E. M., Stricker, J., Gardel, M. and Mogilner, A.** (2015). Model for adhesion clutch explains biphasic relationship between actin flow and traction at the cell leading edge. *Phys. Biol.* **12**, 035002. doi:10.1088/1478-3975/12/3/035002
- Cuvelier, D., Théry, M., Chu, Y.-S., Dufour, S., Thiéry, J.-P., Bornens, M., Nassoy, P. and Mahadevan, L.** (2007). The universal dynamics of cell spreading. *Curr. Biol.* **17**, 694–699. doi:10.1016/j.cub.2007.02.058
- Deserno, M.** (2015). Fluid lipid membranes: From differential geometry to curvature stresses. *Chem. Phys. Lipids.* **185**, 11–45. doi:10.1016/j.chemphyslip.2014.05.001
- Dimilla, P. A., Barbee, K. and Lauffenburger, D. A.** (1991). Mathematical model for the effects of adhesion and mechanics on cell migration speed. *Biophys. J.* **60**, 15–37. doi:10.1016/S0006-3495(91)82027-6
- Djannatian, M., Timmler, S., Arends, M., Luckner, M., Weil, M.-T., Alexopoulos, I., Snaidero, N., Schmid, B., Misgeld, T., Möbius, W. et al.** (2019). Two adhesive systems cooperatively regulate axon ensheathment and myelin growth in the CNS. *Nat. Commun.* **10**, 4794. doi:10.1038/s41467-019-12789-z
- Döbereiner, H. G., Dubin-Thaler, B., Giannone, G., Xenias, H. S. and Sheetz, M. P.** (2004). Dynamic phase transitions in cell spreading. *Phys. Rev. Lett.* **93**, 108105. doi:10.1103/PhysRevLett.93.108105
- Drab, M., Sadhu, R. K., Ravid, Y., Igljić, A., Kralj-Igljić, V. and Gov, N. S.** (2023). Modeling cellular shape changes in the presence of curved membrane proteins and active cytoskeletal forces. In *Plasma Membrane Shaping* (Ed: Shiro Suetsugu), pp. 415–429. Academic Press. doi:10.1016/B978-0-323-89911-6.00002-9
- Driscoll, M. K., Mccann, C., Kopace, R., Homan, T., Fourkas, J. T., Parent, C. and Losert, W.** (2012). Cell shape dynamics: from waves to migration. *PLoS Comput. Biol.* **8**, e1002392. doi:10.1371/journal.pcbi.1002392
- Driscoll, M. K., Sun, X., Guven, C., Fourkas, J. T. and Losert, W.** (2014). Cellular contact guidance through dynamic sensing of nanotopography. *ACS Nano* **8**, 3546–3555. doi:10.1021/nn406637c
- Flannagan, R. S., Jaumouillé, V. and Grinstein, S.** (2012). The cell biology of phagocytosis. *Annu. Rev. Pathol. Mech. Dis.* **7**, 61–98. doi:10.1146/annurev-pathol-011811-132445
- Flemming, S., Font, F., Alonso, S. and Beta, C.** (2020). How cortical waves drive fission of motile cells. *Proc. Natl. Acad. Sci. USA* **117**, 6330–6338. doi:10.1073/pnas.1912428117
- Fošnarič, M., Penič, S., Igljić, A., Kralj-Igljić, V., Drab, M. and Gov, N. S.** (2019). Theoretical study of vesicle shapes driven by coupling curved proteins and active cytoskeletal forces. *Soft Mat.* **15**, 5319–5330. doi:10.1039/C8SM02356E
- Frey, F. and Idema, T.** (2021). More than just a barrier: using physical models to couple membrane shape to cell function. *Soft Mat.* **17**, 3533–3549. doi:10.1039/D0SM01758B
- Fritz-Laylin L. K., Riel-Mehan M., Chen B. C., Lord S. J., Goddard T. D., Ferrin T. E., Nicholson-Dykstra S. M., Higgs H., Johnson G. T. et al.** (2017). Actin-based protrusions of migrating neutrophils are intrinsically lamellar and facilitate direction changes. *Elife* **6**, e26990. doi:10.7554/eLife.26990
- Gardel, M. L., Schneider, I. C., Aratyn-Schaus, Y. and Waterman, C. M.** (2010). Mechanical integration of actin and adhesion dynamics in cell migration. **26**, 315–333. doi:10.1146/annurev.cellbio.011209.122036
- Giardini, P. A., Fletcher, D. A. and Theriot, J. A.** (2003). Compression forces generated by actin comet tails on lipid vesicles. *Proc. Natl. Acad. Sci. USA* **100**, 6493–6498. doi:10.1073/pnas.1031670100
- Gov, N. S.** (2018). Guided by curvature: Shaping cells by coupling curved membrane proteins and cytoskeletal forces. *Philos. Trans. R. Soc. B: Biol. Sci.* **373**, 20170115. doi:10.1098/rstb.2017.0111
- Graziano, B. R., Town, J. P., Sitarska, E., Nagy, T. L., Fošnarič, M., Penič, S., Igljić, A., Kralj-Igljić, V., Gov, N. S., Diz-Muñoz, A. et al.** (2019). Cell confinement reveals a branched-actin independent circuit for neutrophil polarity. *PLoS Biol.* **17**, e3000457. doi:10.1371/journal.pbio.3000457
- Guetta-Terrier, C., Monzo, P., Zhu, J., Long, H., Venkatraman, L., Zhou, Y., Wang, P. P., Chew, S. Y., Mogilner, A., Ladoux, B. et al.** (2015). Protrusive waves guide 3D cell migration along nanofibers. *J. Cell Biol.* **211**, 683–701. doi:10.1083/jcb.201501106
- Guo, M., Pegoraro, A. F., Mao, A., Zhou, E. H., Arany, P. R., Han, Y., Burnette, D. T., Jensen, M. H., Kasza, K. E., Moore, J. R. et al.** (2017). Cell volume change through water efflux impacts cell stiffness and stem cell fate. *Proc. Natl. Acad. Sci. USA* **114**, E8618–E8627. doi:10.1073/pnas.1705179114
- He, X. and Jiang, Y.** (2017). Substrate curvature regulates cell migration. *Phys. Biol.* **14**, 035006. doi:10.1088/1478-3975/aa6f18e
- Helfrich, W.** (1974). Blocked lipid exchange in bilayers and its possible influence on the shape of vesicles. *Z. Naturforsch C J Biosci.* **29**, 510–515. doi:10.1515/znc-1974-9-1010
- Honda, G., Saito, N., Fujimori, T., Hashimura, H., Nakamura, M. J., Nakajima, A. and Sawai, S.** (2021). Microtopographical guidance of macropinocytic signaling patches. *Proc. Natl. Acad. Sci. USA* **118**, e2110281118. doi:10.1073/pnas.2110281118.

- Hu, L. and Papoian, G. A. (2010). Mechano-chemical feedbacks regulate actin mesh growth in lamellipodial protrusions. *Biophys. J.* **98**, 1375-1384. doi:10.1016/j.bpj.2009.11.054
- Hwang, C. M., Park, Y., Park, J. Y., Lee, K., Sun, K., Khademhosseini, A. and Lee, S. H. (2009). Controlled cellular orientation on PLGA microfibers with defined diameters. *Biomed. Microdevices* **11**, 739-746. doi:10.1007/s10544-009-9287-7
- Innocenti, M. (2018). New insights into the formation and the function of lamellipodia and ruffles in mesenchymal cell migration. *Cell Adh. Migr.* **12**, 401-416. doi:10.1080/19336918.2018.1448352
- Kabaso, D., Bobrovska, N., Gózdź, W., Gov, N., Kralj-Iglič, V., Veranič, P. and Iglič, A. (2012). On the role of membrane anisotropy and BAR proteins in the stability of tubular membrane structures. *J. Biomech.* **45**, 231-238. doi:10.1016/j.jbiomech.2011.10.039
- Kennedy, K. M., Bhaw-Luximon, A. and Jhurry, D. (2017). Cell-matrix mechanical interaction in electrospun polymeric scaffolds for tissue engineering: Implications for scaffold design and performance. *Acta Biomater.* **50**, 41-55. doi:10.1016/j.actbio.2016.12.034
- Koenderink, G. H. and Paluch, E. K. (2018). Architecture shapes contractility in actomyosin networks. *Curr. Opin. Cell Biol.* **50**, 79-85. doi:10.1016/j.cob.2018.01.015
- Koons, B., Sharma, P., Ye, Z., Mukherjee, A., Lee, M. H., Wirtz, D., Behkam, B. and Nain, A. S. (2017). Cancer protrusions on a tightrope: nanofiber curvature contrast quantitates single protrusion dynamics. *ACS Nano* **11**, 12037-12048. doi:10.1021/acsnano.7b04567
- Kumari, S., Mg, S. and Mayor, S. (2010). Endocytosis unplugged: multiple ways to enter the cell. *Cell* **20**, 256-275. doi:10.1038/cr.2010.19
- Le Clairche, C. and Carlier, M. F. (2008). Regulation of actin assembly associated with protrusion and adhesion in cell migration. *Physiol. Rev.* **88**, 489-513. doi:10.1152/physrev.00021.2007
- Link, R., Weißenbruch, K., Tanaka, M., Bastmeyer, M. and Schwarz, U. S. (2023). Cell shape and forces in elastic and structured environments: from single cells to organoids. *Adv. Funct. Mater. [In press]*. doi:10.1002/adfm.202302145
- Li, Y., Lovett, D., Zhang, Q., Neelam, S., Kuchibhotla, R. A., Zhu, R., Gunderson, G. G., Lele, T. P. and Dickinson, R. B. (2015). Moving cell boundaries drive nuclear shaping during cell spreading. *Biophys. J.* **109**, 670-686. doi:10.1016/j.bpj.2015.07.006
- Liu, A. P., Richmond, D. L., Maibaum, L., Pronk, S., Geissler, P. L. and Fletcher, D. A. (2008). Membrane-induced bundling of actin filaments. *Nat. Phys.* **4**, 789. doi:10.1038/nphys1071
- Liu, S., Xiong, X., Zhao, X., Yang, X. and Wang, H. (2015). F-BAR family proteins, emerging regulators for cell membrane dynamic changes - From structure to human diseases. *J. Hematol. Oncol.* **8**, 47. doi:10.1186/s13045-015-0144-2
- Machesky, L. M., Mullins, R. D., Higgs, H. N., Kaiser, D. A., Blanchoin, L., May, R. C., Hall, M. E. and Pollard, T. D. (1999). Scar, a WASP-related protein, activates nucleation of actin filaments by the Arp2/3 complex. *Proc. Natl. Acad. Sci. USA* **96**, 3739-3744. doi:10.1073/pnas.96.7.3739
- Maiuri, P., Rupprecht, J.-F., Wieser, S., Rupprecht, V., Bénichou, O., Carpi, N., Coppey, M., De Beco, S., Gov, N., Heisenberg, C.-P. et al. (2015). Actin flows mediate a universal coupling between cell speed and cell persistence. *Cell* **161**, 374-386. doi:10.1016/j.cell.2015.01.056
- Mattila Pietä, K. and Lappalainen, P. (2008). Filopodia: molecular architecture and cellular functions. *Nat. Rev. Mol. Cell Biol.* **9**, 446-454. doi:10.1038/nrm2406
- McMahon, H. T. and Boucrot, E. (2015). Membrane curvature at a glance. *J. Cell Sci.* **128**, 1065-1070. doi:10.1242/jcs.114454
- McMahon, H. T. and Gallop, J. L. (2005). Membrane curvature and mechanisms of dynamic cell membrane remodelling. *Nature* **438**, 590. doi:10.1038/nature04396
- Meehan, S. and Nain, A. S. (2014). Role of suspended fiber structural stiffness and curvature on single-cell migration, nucleus shape, and focal-adhesion-cluster length. *Biophys. J.* **107**, 2604-2611. doi:10.1016/j.bpj.2014.09.045
- Mesarec, L., Drab, M., Penič, S., Kralj-Iglič, V. and Iglič, A. (2021). On the role of curved membrane nanodomains and passive and active skeleton forces in the determination of cell shape and membrane budding. *Int. J. Mol. Sci.* **22**, 2348. doi:10.3390/ijms22052348
- Mesarec, L., Gózdź, W., Kralj-Iglič, V., Kralj, S. and Iglič, A. (2023). Coupling of nematic in-plane orientational ordering and equilibrium shapes of closed flexible nematic shells. *Sci. Rep.* **13**, 10663. doi:10.1038/s41598-023-37664-2
- Mogilner, A. and Oster, G. (1996). Cell motility driven by actin polymerization. *Biophys. J.* **71**, 3030-3045. doi:10.1016/S0006-3495(96)79496-1
- Mogilner, A. and Oster, G. (2003). Force generation by actin polymerization II: the elastic ratchet and tethered filaments. *Biophys. J.* **84**, 1591-1605. doi:10.1016/S0006-3495(03)74969-8
- Mori, Y., Jilkine, A. and Edelstein-Keshet, L. (2008). Wave-pinning and cell polarity from a bistable reaction-diffusion system. *Biophys. J.* **94**, 3684-3697. doi:10.1529/biophysj.107.120824
- Mukherjee, A., Behkam, B. and Nain, A. S. (2019). Cancer cells sense fibers by coiling on them in a curvature-dependent manner. *iScience* **19**, 905-915. doi:10.1016/j.isci.2019.08.023
- Mylvaganam, S., Freeman, S. A. and Grinstein, S. (2021). The cytoskeleton in phagocytosis and macropinocytosis. *Curr. Biol.* **31**, R619-R632. doi:10.1016/j.cub.2021.01.036
- Naoz, M., Manor, U., Sakaguchi, H., Kachar, B. and Gov, N. S. (2008). Protein localization by actin treadmill and molecular motors regulates stereocilia shape and treadmill rate. *Biophys. J.* **95**, 5706-5718. doi:10.1529/biophysj.108.143453
- Niedergang, F. and Chavrier, P. (2004). Signaling and membrane dynamics during phagocytosis: many roads lead to the phagos(R)ome. *Curr. Opin. Cell Biol.* **16**, 422-428. doi:10.1016/j.cob.2004.06.006
- Orly, G., Manor, U. and Gov, N. S. (2015). A biophysical model for the staircase geometry of stereocilia. *PLoS One* **10**, e0127926. doi:10.1371/journal.pone.0127926
- Pawluchin, A. and Galic, M. (2022). Moving through a changing world: single cell migration in 2D vs. 3D. *Front Cell Dev Biol.* **10**, 1080995. doi:10.3389/fcell.2022.1080995
- Pieuchot, L., Marteau, J., Guignandon, A., Dos Santos, T., Brigaud, I., Chauvy, P.-F., Cloatre, T., Ponche, A., Petithory, T., Rougerie, P. et al. (2018). Curvotaxis directs cell migration through cell-scale curvature landscapes. *Nat. Commun.* **9**, 3995. doi:10.1038/s41467-018-06494-6
- Pipathsouk, A., Brunetti, R. M., Town, J. P., Graziano, B. R., Breuer, A., Pellett, P. A., Marchuk, K., Tran, N.-H. T., Krummel, M. F., Stamou, D. et al. (2021). The WAVE complex associates with sites of saddle membrane curvature. *J. Cell Biol.* **220**, e202003086. doi:10.1083/jcb.202003086
- Pollard, T. D. and Cooper, J. A. (2009). Actin, a central player in cell shape and movement. *Science (1979)* **326**, 1208-1212. doi:10.1126/science.1175862
- Pollitt, A. Y. and Insall, R. H. (2009). WASP and SCAR/WAVE proteins: the drivers of actin assembly. *J. Cell Sci.* **122**, 2575-2578. doi:10.1242/jcs.023879
- Ravid, Y., Penič, S., Mimori-Kiyosue, Y., Suetsugu, S., Iglič, A. and Gov, N. S. (2023). Theoretical model of membrane protrusions driven by curved active proteins. *Front. Mol. Biosci.* **10**, 301. doi:10.3389/fmolb.2023.1153420
- Richards, D. M. and Endres, R. G. (2017). How cells engulf: a review of theoretical approaches to phagocytosis. *Rep. Prog. Phys.* **80**, 126601. doi:10.1088/1361-6633/aa8730
- Sackmann, E. and Smith, A. S. (2014). Physics of cell adhesion: some lessons from cell-mimetic systems. *Soft Mat.* **10**, 1644-1659. doi:10.1039/c3sm51910d
- Sadhu, R. K., Penič, S., Iglič, A. and Gov, N. S. (2021). Modelling cellular spreading and emergence of motility in the presence of curved membrane proteins and active cytoskeleton forces. *Eur. Phys. J. Plus* **136**, 495. doi:10.1140/epjp/s13360-021-01433-9
- Sadhu, R. K., Barger, S. R., Penič, S., Iglič, A., Krendel, M., Gauthier, N. C. and Gov, N. S. (2022). A theoretical model of efficient phagocytosis driven by curved membrane proteins and active cytoskeleton forces. *Soft Mat.* **19**, 31-43. doi:10.1039/D2SM01152B
- Sadhu, R. K., Hernandez-Padilla, C., Eisenbach, Y. E., Zhang, L., Vishwasrao, H. D., Behkam, B., Shroff, H., Iglič, A., Peles, E., Nain, A. S. et al. (2023a). Coiling of cellular protrusions around extracellular fibers. *Nature Commun.* (in press).
- Sadhu, R. K., Luciano, M., Xi, W., Martinez-Torres, C., Schröder, M., Blum, C., Tarantola, M., Penič, S., Iglič, A., Beta, C. et al. (2023b). A minimal physical model for curvotaxis driven by curved protein complexes at the cell's leading edge. *bioRxiv*. doi:10.1101/2023.04.19.537490
- Sadhukhan, S., Penic, S., Iglič, A. and Gov, N. S. (2023). Modelling how curved active proteins and shear flow pattern cellular shape and motility. *Front. Cell Dev. Biol.* **11**, 600. doi:10.3389/fcell.2023.1193793
- Safran, S. A. (2003). *Statistical Thermodynamics of Surfaces, Interfaces, and Membranes*. Westview Press.
- Saito, N. and Sawai, S. (2021). Three-dimensional morphodynamic simulations of macropinocytic cups. *iScience* **24**, 103087. doi:10.1016/j.isci.2021.103087
- Salbreux, G., Charras, G. and Paluch, E. (2012). Actin cortex mechanics and cellular morphogenesis. *Trends Cell Biol.* **22**, 536-545. doi:10.1016/j.tcb.2012.07.001
- Sanz-Herrera, J. A., Moreo, P., García-Aznar, J. M. and Doblaré, M. (2009). On the effect of substrate curvature on cell mechanics. *Biomaterials* **30**, 6674-6686. doi:10.1016/j.biomaterials.2009.08.053
- Sauvanet, C., Wayt, J., Pelaseyed, T. and Bretscher, A. (2015). Structure, regulation, and functional diversity of microvilli on the apical domain of epithelial cells. *Annu. Rev. Cell Dev. Biol.* **31**, 593-621. doi:10.1146/annurev-cellbio-100814-125234
- Schamberger, B., Ziege, R., Anselme, K., Ben Amar, M., Bykowski, M., Castro, A. P. G., Cipitria, A., Coles, R. A., Dimova, R., Eder, M. et al. (2023). Curvature in biological systems: its quantification, emergence, and implications across the scales. *Adv. Mater.* **35**, e2206110. doi:10.1002/adma.202206110
- Schwarz, U. S. and Safran, S. A. (2013). Physics of adherent cells. *Rev. Mod. Phys.* **85**, 1327-1381. doi:10.1103/RevModPhys.85.1327
- Serpelloni, M., Arricca, M., Bonanno, C. and Salvadori, A. (2021). Modeling cells spreading, motility, and receptors dynamics: a general framework. *Acta Mech. Sin.* **37**, 1013-1030. doi:10.1007/s10409-021-01088-w
- Song, K. H., Park, S. J., Kim, D. S. and Doh, J. (2015). Sinusoidal wavy surfaces for curvature-guided migration of Tlymphocytes. *Biomaterials* **51**, 151-160. doi:10.1016/j.biomaterials.2015.01.071

- Spence, H. J., Timpson, P., Tang, H. R., Insall, R. H. and Machesky, L. M. (2012). Scar/WAVE3 contributes to motility and plasticity of lamellipodial dynamics but not invasion in three dimensions. *Biochem. J.* **448**, 35–42. doi:10.1042/BJ20112206
- Stadelmann, C., Timmler, S., Barrantes-Freer, A. and Simons, M. (2019). Myelin in the central nervous system: Structure, function, and pathology. *Physiol. Rev.* **99**, 1381–1431. doi:10.1152/physrev.00031.2018
- Stradal, T. E. B., Rottner, K., Disanza, A., Confalonieri, S., Innocenti, M. and Scita, G. (2004). Regulation of actin dynamics by WASP and WAVE family proteins. *Trends Cell Biol.* **14**, 303–311. doi:10.1016/j.tcb.2004.04.007
- Streicher, P., Nassoy, P., Bärmann, M., Dif, A., Marchi-Artzner, V., Brochard-Wyart, F., Spatz, J. and Bassereau, P. (2009). Integrin reconstituted in GUVs: A biomimetic system to study initial steps of cell spreading. *Biochim. Biophys. Acta (BBA) – Biomembr.* **1788**, 2291–2300. doi:10.1016/j.bbmem.2009.07.025
- Svitkina, T. M., Rovinsky, Y. A., Bershadsky, A. D. and Vasiliev, J. M. (1995). Transverse pattern of microfilament bundles induced in epitheliocytes by cylindrical substrata. *J. Cell Sci.* **108**, 735–745. doi:10.1242/jcs.108.2.735
- Szeczyk, D., Yamamoto, T. and Riveline, D. (2013). Non-monotonic relationships between cell adhesion and protrusions. *New J. Phys.* **15**, 035031. doi:10.1088/1367-2630/15/3/035031
- Takenawa, T. and Miki, H. (2001). WASP and WAVE family proteins: key molecules for rapid rearrangement of cortical actin filaments and cell movement. *J. Cell Sci.* **114**, 1801–1809. doi:10.1242/jcs.114.10.1801
- Tamemoto, N. and Noguchi, H. (2020). Pattern formation in reaction–diffusion system on membrane with mechanochemical feedback. *Sci. Rep.* **10**, 19582. doi:10.1038/s41598-020-76695-x
- Tamemoto, N. and Noguchi, H. (2021). Reaction-diffusion waves coupled with membrane curvature. *Soft Mat.* **17**, 6589–6596. doi:10.1039/D1SM00540E
- Taniguchi, D., Ishihara, S., Oonuki, T., Honda-Kitahara, M., Kaneko, K. and Sawai, S. (2013). Phase geometries of two-dimensional excitable waves govern self-organized morphodynamics of amoeboid cells. *Proc. Natl. Acad. Sci. USA* **110**, 5016–5021. doi:10.1073/pnas.1218025110
- Upadhyaya, A., Chabot, J. R., Andreeva, A., Samadani, A. and Van Oudenaarden, A. (2003). Probing polymerization forces by using actin-propelled lipid vesicles. *Proc. Natl. Acad. Sci. USA* **100**, 4521–4526. doi:10.1073/pnas.0837027100
- Vassaux, M., Pieuchot, L., Anselme, K., Bigerelle, M. and Milan, J. L. (2019). A biophysical model for curvature-guided cell migration. *Biophys. J.* **117**, 1136–1144. doi:10.1016/j.bpj.2019.07.022
- Vorselen, D., Barger, S. R., Wang, Y., Cai, W., Theriot, J. A., Gauthier, N. C. and Krendel, M. (2021). Phagocytic “teeth” and myosin-ii “jaw” power target constriction during phagocytosis. *Elife* **10**, e68627. doi:10.7554/eLife.68627
- Welch, M. D. and Mullins, R. D. (2002). Cellular control of actin nucleation. *Annu. Rev. Cell Dev. Biol.* **18**, 247–288. doi:10.1146/annurev.cellbio.18.040202.112133
- Werner, M., Kurniawan, N. A., Korus, G., Bouten, C. V. C. and Petersen, A. (2018). Mesoscale substrate curvature overrules nanoscale contact guidance to direct bone marrow stromal cell migration. *J. R. Soc. Interface* **15**, 20180162. doi:10.1098/rsif.2018.0162
- Werner, M., Petersen, A., Kurniawan, N. A. and Bouten, C. V. C. (2019). Cell-perceived substrate curvature dynamically coordinates the direction, speed, and persistence of stromal cell migration. *Adv. Biosyst.* **3**, 1900080. doi:10.1002/adbi.201900080
- Werner, M., Kurniawan, N. A. and Bouten, C. V. C. (2020). Cellular geometry sensing at different length scales and its implications for scaffold design. *Materials* **13**, 963. doi:10.3390/ma13040963
- Winkler, B., Aranson, I. S. and Ziebert, F. (2019). Confinement and substrate topography control cell migration in a 3D computational model. *Commun. Phys.* **2**, 82. doi:10.1038/s42005-019-0185-x
- Wu, M. and Liu, J. (2021). Mechanobiology in cortical waves and oscillations. *Curr. Opin. Cell Biol.* **68**, 45–54. doi:10.1016/j.ceb.2020.08.017
- Xiong, Y., Rangamani, P., Fardin, M., Lipshtat, A., Dubin-Thaler, B., Rossier, O., Sheetz, M. P. and Iyengar, R. (2010). Mechanisms controlling cell size and shape during isotropic cell spreading. *Biophys. J.* **98**, 2136–2146. doi:10.1016/j.bpj.2010.01.059
- Zimmerberg, J. and Kozlov, M. M. (2006). How proteins produce cellular membrane curvature. *Nat. Rev. Mol. Cell Biol.* **7**, 9–19. doi:10.1038/nrm1784
- Zhu, Z. and Bhat, K. M. (2011). The Hem protein mediates neuronal migration by inhibiting WAVE degradation and functions opposite of Abelson tyrosine kinase. *Dev. Biol.* **357**, 283–294. doi:10.1016/j.ydbio.2011.06.025